J. Biochem. **137**, 303–314 (2005)
DOI: 10.1093/jb/mvi033

Structural and Functional Characterization of Rabbit and Human L-Gulonate 3-Dehydrogenase

Syuhei Ishikura[1], Noriyuki Usami[2], Mayuko Araki[1] and Akira Hara[1,*]

[1]Laboratory of Biochemistry, Gifu Pharmaceutical University, Mitahora-higashi, Gifu 502-8585; and [2]Faculty of Health Science, Kyusyuu University of Health and Welfare, Nobeoka, Miyazaki 822-8508

Received November 15, 2004; accepted December 17, 2004

L-Gulonate 3-dehydrogenase (GDH) catalyzes the NAD^+-linked dehydrogenation of L-gulonate into dehydro-L-gulonate in the uronate cycle. In this study, we isolated the enzyme and its cDNA from rabbit liver, and found that the cDNA is identical to that for rabbit lens λ-crystallin except for lacking a codon for Glu^{309}. The same cDNA species, but not the λ-crystallin cDNA with the codon for Glu^{309}, was detected in the lens, which showed the highest GDH activity among rabbit tissues. In addition, recombinant human λ-crystallin that lacks Glu^{309} displays enzymatic properties similar to rabbit GDH. These data indicate that GDH is recruited as λ-crystallin without gene duplication. An outstanding feature of GDH is modulation of its activity by low concentrations of P_i, which decreases the catalytic efficiency in a dose dependent manner. P_i also protects the enzyme against both thermal and urea denaturation. Kinetic analysis suggests that P_i binds to both the free enzyme and its NAD(H)-complex in the sequential ordered mechanism. Furthermore, we examined the roles of Asp^{36}, Ser^{124}, His^{145}, Glu^{157} and Asn^{196} in the catalytic function of rabbit GDH by site-directed mutagenesis. The D36R mutation leads to a switch in favor of NADP(H) specificity, suggesting an important role of Asp^{36} in the coenzyme specificity. The S124A mutation decreases the catalytic efficiency 500-fold, and the H145Q, N196Q and N195D mutations result in inactive enzyme forms, although the E157Q mutation produces no large kinetic alteration. Thus, Ser^{124}, His^{145} and Asn^{196} may be critical for the catalytic function of GDH.

Key words: λ-crystallin, L-gulonate 3-dehydrogenase, 3-hydroxyacyl CoA dehydrogenase, inorganic phosphate, uronate cycle.

Abbreviations used: λ-CRY, λ-crystallin; GDH, L-gulonate 3-dehydrogenase; HAD, 3-hydroxyacyl CoA dehydrogenase; HBA, L-3-hydroxybutyrate; 2-ME, 2-mercaptoethanol; RT, reverse transcription.

The uronate cycle, an alternative glucose metabolic pathway that is linked to the pentose phosphate cycle *via* non-phosphorylated sugar metabolites, plays essential roles in glucuronide formation and the synthesis of glycosaminoglycan and ascorbic acid. Additionally, recent studies on L-xylulose reductase and other enzymes in this cycle suggested roles in osmoregulation, the prevention of osmolytic stress in the renal tubules and lens by producing the osmolyte xylitol, and the detoxification of reactive α-dicarbonyls and short-chain sugars (*1*, *2*). In mammals other than primates and guinea pig, L-gulonate formed in the uronate cycle is incorporated in the branched pathway to yield ascorbic acid, and it may thereby be possible that there are some control systems for the two pathways, *i.e.*, the uronate cycle and ascorbic acid formation, at either or both of the enzymes that catalyze the first steps of the two pathways. Such enzymes are L-gulonate 3-dehydrogenase (GDH, EC 1.1.1.45) in the uronate cycle (*3*) and gluconolactonase in the ascorbic acid synthesis pathway (*4*), but there have been no reports on the metabolic regulation of the two enzymes. The properties of gluconolactonases of pig and bovine liver (*5–7*) are well-characterized, and the sequences of genes for the microbial enzymes have been deposited in a DNA data bank. Mammalian GDH has been partially purified from pig liver, and designated as L-hydroxyacid dehydrogenase because of its substrate specificity for several L-hydroxyacids (*3*), but its properties, structure and tissue distribution are largely unknown.

In this study, we have isolated GDH and its cDNA from rabbit liver in order to elucidate its structural and enzymatic characteristics including endogenous compounds that influence the enzyme activity. The data show that the primary structure of rabbit GDH is identical to that of a toxon-specific λ-crystallin (λ-CRY) (*8*). Counterparts of the rabbit λ-CRY cDNA have recently been cloned from non-lenticular tissues of man, rat, mouse and cow (*9*), but the physiological functions of the proteins encoded in the cDNAs remain unknown. Therefore, we also examined the enzymatic properties of recombinant human λ-CRY and provide evidence for the identity of λ-CRY and GDH. In the characterization of both the rabbit and human enzymes, inorganic phosphate (P_i) was found to act as a modulator of enzyme activity as well as a stabilizer against both thermal and urea denaturation of the enzymes. Rabbit and human GDHs show low amino acid sequence identity (about 22%) only with 3-hydroxyacyl CoA dehydrogenase (HAD) of the oxidoreductases in the

*To whom correspondence should be addressed. Phone/Fax: +81-58237-8586, E-mail: hara@gifu-pu.ac.jp

protein databases. Despite of low sequence similarity, GDH possesses the same residues for coenzyme-binding (Asp^{36}) and in the active site (Ser^{124}, His^{145}, Gln^{157} and Asn^{196}) as found in the crystal structure of human HAD (*10*, *11*). Furthermore, we examined the effects of site-directed mutagenesis of the five residues on the catalytic function of rabbit GDH to elucidate the structural relationship between GDH and HAD.

MATERALS AND METHODS

Materials—L-Gulonic acid (*12*), dehydroascorbic acid, 2,3-diketogulonic acid (*13*), and 3-deoxyglucosone (*14*) were synthesized as described previously. Other sugars and compounds tested as substrates and inhibitors were obtained from Sigma-Aldrich (St. Louis, USA), Fluka Chemie (Buchs, Switzerland), and Tokyo Kasei Organic Chemicals (Tokyo, Japan). Pyridine nucleotide coenzymes and pI markers were obtained from Oriental Yeast (Tokyo, Japan); a pCR T7/CT-TOPO TA expression kit, Superscript II, an oligo dT primer and *Escherichia coli* BL21 (DE3) pLysS were from Invitrogen (Carlsbad, CA, USA); *Pfu* DNA polymerase, total RNA of human liver and a QuickChange™ site-directed mutagenesis kit were from Stratagene (La Jolla, CA, USA); and *Taq* DNA polymerase was from Takara (Kusatsu, Japan). Matrex Green A and phosphate-cellulose were purchased from Amicon (Beverly, MA, USA) and Whatman (Maidstone, Kent, UK), respectively, and other resins for column chromatography were from Amersham Biosciences (Piscataway, NJ, USA). All other chemicals were of the highest grade that could be obtained commercially.

Purification of GDH—The following procedures for purification of the enzyme were performed at 4°C; buffers were supplemented with 5 mM 2-mercaptoethanol (2-ME) to stabilize the enzyme. The liver (50 g) of a male Japanese white rabbit was homogenized in 4 volumes of 0.25 M sucrose containing 20 mM Tris-HCl, pH 7.5, using a Potter-Elvejhem homogenizer, and the homogenate was centrifuged at 105,000 × *g* for 1 h. The portion of the supernatant fraction that precipitated between 35 and 70% $(NH_4)_2SO_4$ saturation was collected by centrifugation at 12,000 × *g* for 15 min, dissolved in 10 mM Tris-HCl, pH 8.0, containing 0.1 M NaCl, and then dialyzed against the same buffer. The dialyzed solution was applied to a Sephadex G-100 column (3 × 70 cm) equilibrated with the same buffer. The GDH fractions were concentrated by ultrafiltration using an Amicon YM-10 membrane, dialyzed against 10 mM Tris-HCl, pH 8.0, and then applied to a Q-Sepharose column (2 × 20 cm) equilibrated with buffer. The enzyme was eluted with a linear gradient of 0–0.1 M NaCl in buffer. The enzyme fractions were dialyzed against 10 mM Tris-HCl, pH 8.0, and applied to a Blue-Sepharose column (1.5 × 10 cm) equilibrated with the same buffer. The column was washed with buffer containing 0.5 mM $NADP^+$, and the enzyme was eluted with buffer containing 0.1 M KCl. The enzyme fraction was dialyzed against 10 mM Tris-HCl, pH 8.0, and applied to a hydroxylapatite column (2 × 15 cm). The adsorbed enzyme was eluted with a linear gradient of 0–0.1 M potassium phosphate, pH 8.0, in the same buffer. The enzyme fraction was dialyzed against 10 mM Mes, pH 6.4, and applied to a phosphate-cellulose column (2 × 5 cm) equilibrated with buffer. The column was first washed with 50 mM Mops, pH 7.0, and the enzyme was eluted with 50 mM pyrophosphate, pH 7.0. The enzyme fractions were dialyzed against 10 mM Tris-HCl, pH 8.0, containing 20% (w/v) glycerol, and stored at –35°C.

cDNA Isolation and Site-Directed Mutagenesis—DNA and RNA techniques were performed as described by Sambrook *et al.* (*15*), and as previously reported (*1*, *16*). Total RNA was extracted from the livers and lenses of rabbits, and subjected to reverse transcription (RT) at 42°C for 50 min using Superscript II and the oligo dT primer. The cDNA for rabbit λ-CRY was amplified from the single-strand cDNAs by PCR using *Pfu* DNA polymerase and primers rgdh1 and rgdh2. rgdh1 corresponds to positions 1–17 of the sequence of rabbit λ-CRY cDNA (*8*), and rgdh2 is complementary to positions 767–783. The cDNA for human λ-CRY was also isolated from a total RNA preparation from human liver by RT-PCR using forward and reverse primers, corresponding to positions 1–17 and 767–786, respectively, of the sequence of human λ-CRY cDNA (*9*). The PCR product was subcloned into the pCR T7/CT-TOPO vector. The sequences of the inserts were determined with a CEQ2000XL DNA sequencer (Beckman Coulter). The nucleotide sequences of the cDNAs for rabbit and human λ-CRYs were verified by repeating RT-PCR.

Mutagenesis was performed with the QuickChange™ site-directed mutagenesis kit according to the protocol described by the manufacturer. The sequences (5′→3′) of the mutagenic primers were cagggtgaagctgtacCGCattgagccacggcag (D36R), ctgagcagttccagcGCCtgcctcctgccctcc (S124A), cagtgcatcgtggccCAGccggtcaacccaccatac (H145Q), catcccgctggtcCAGctggtcccacacccagag (E157Q), gatggcttcgtgctcCAGcgcctgcagtacgccatc (N196Q), and gatggcttcgtgctcGACcgcctgcagtacgccatc (N196D), where the mutated codons are shown in capital letters. The complete coding regions of the cDNAs were sequenced to confirm the presence of the desired mutation and to ensure that no other mutation had occurred.

Expression and Purification of Recombinant Proteins—To express the recombinant proteins, the *E. coli* cells were transformed with the pCR T7/CT-TOPO vector harboring the cDNA for rabbit or human λ-CRY. The *E. coli* cells were cultured in LB medium containing ampicillin (50 μg/ml) at 37°C until the absorbance at 600 nm reached 0.5. Then isopropyl 1-thio-β-D-galactoyranoside (1 mM) was added to induce the expression of the recombinant enzyme, and the culture was continued for 6 h at 37°C for rabbit λ-CRY. For the expression of human λ-CRY, the time and temperature of induction were changed to 12 h and 25°C, respectively. Cell extracts were prepared as described previously (*1*, *16*). Recombinant rabbit λ-CRY and its mutants were purified according to the purification procedure for rabbit liver GDH, and homogenous preparations were obtained at the Blue-Sepharose column step. During their purification, the H145Q and N196Q mutant enzymes with no catalytic activity were detected by SDS-PAGE (*17*) in 12.5% (w/v) gels with Coomassie Brilliant Blue staining, and confirmed by Western blotting (*18*) using an antibody against rabbit GDH raised in rats. For purification of the recombinant human λ-CRY, DEAE-Sephacel and Matrex

Green A were employed as the column resins instead of Q-Sepharose and Blue-Sepharose. The enzyme fraction obtained by Sephadex G-100 chromatography was diluted with the same volume of 10 mM Tris-HCl, pH 8.0, and then applied to a DEAE-Sepharose column (1.8 × 30 cm) equilibrated with the same buffer containing 50 mM NaCl. The column was washed with 20 mM potassium phosphate, pH 7.0, and the enzyme was eluted with a linear gradient of 0–0.12 M NaCl in the same buffer. The enzyme fraction was dialyzed against 20 mM potassium phosphate, pH 6.5, and then applied to a Matrex Green A column (2 × 15 cm) equilibrated with the same buffer. The column was washed with buffer, and the enzyme was eluted with 20 mM potassium phosphate, pH 7.0.

Assay of GDH Activity—The dehydrogenase and reductase activities of GDH were assayed by measuring the rate of change in NADH absorbance at 340 nm. The standard reaction mixture for dehydrogenase activity consisted of 50 mM Mops, pH 7.0, 1 mM NAD^+, 10 mM L-gulonate and enzyme, in a total volume of 2.0 ml. The activity in the *E. coli* extract and during the purification was assayed with Tris-HCl, pH 8.5, instead of the Mops buffer. Additionally, the low dehydrogenase activity of the S124A mutant was determined by measuring the rate of change in NADH fluorescence at 445 nm (excitation at 340 nm). Reductase activity was determined with 0.1 mM NADH and 20 mM acetoacetate as the coenzyme and substrate, respectively, unless otherwise noted. One unit of enzyme activity was defined as the amount of enzyme that catalyzed the reduction and formation of 1 μmol of NADH per min at 25°C.

The pH dependency of the enzyme reaction was analyzed using the following 50 mM buffers: Mes (pH 5.5 and 6.0), Mops (pH 7.0 and 7.5), Tris-HCl (pH 7.5–9.0), and glycine-NaOH (pH 8.5–11.0). In the inhibition studies, the compounds tested as inhibitors were dissolved in water, and the solutions of acidic compounds were neutralized to about pH 7.0 with NaOH. L-Ascorbate was dissolved in 1 mM dithiothreitol to prevent its conversion into a free radical intermediate, monodehydroascorbate (*19*). The inhibitor concentration giving 50% inhibition (IC_{50}) was determined over a range of four inhibitor concentrations. The apparent K_m and V_{max} values were determined over a range of five substrate concentrations at saturating concentration of coenzyme by fitting the initial velocities to the Michaelis-Menten equation. Kinetic studies in the presence of inhibitors or effectors were carried out in a similar manner. The inhibition constant, K_i, was calculated by using the appropriate programs of EnzFitter (Biosoft, Cambridge, UK). The kinetic mechanism and constants of oxidoreduction by the enzyme were analyzed according to the method of Cleland (*20*). The initial velocities were fitted to the equation

$$v = VAB/(AB + K_AB + K_BA + K_{IA}K_B)$$

where v is the initial velocity, V the maximum velocity at saturating substrate concentrations, A and B the two substrate concentrations, K_A and K_B the corresponding Michaelis constants, and K_{IA} the dissociation constant of substrate A. The kinetic constants are the means of triplicate determinations, in which all standard errors of fits were less than 15%, unless otherwise noted.

Stability Study—For thermal inactivation, the enzymes (6 μg/ml) were incubated at 48 or 55°C in buffer A (50 mM Mops, pH 7.0, 10 mM 2-ME and 0.2% bovine serum albumin) in the presence or absence of NAD^+ and/or potassium phosphate, pH 7.0. At different times, aliquots of 25 μl of each sample were taken and assayed for GDH activity. For denaturation with urea, the enzymes (12 μg/ml) were incubated at 25°C for 30 min in buffer A containing 0–4 M urea in the presence or absence of NAD^+ and/or potassium P_i, pH 7.0. For analysis of pH stability, the enzymes (6 μg/ml) were incubated at 25°C for 30 min in the following 50 mM buffers containing 10 mM 2-ME and 0.2% bovine serum albumin: glycine-HCl (pH 3.0 and 3.5), acetate-NaOH (pH 4.0, 4.5 and 5.0), Mes (pH 5.5 and 6.0), Mops (pH 7.0), Tris-HCl (pH 8.0), and glycine-NaOH (pH 9.0, 10.0, 10.5 and 11.0). The remaining activity was expressed as a percentage of the activity of a sample incubated in the absence of urea or without incubation. The enzyme activity was unaffected by the presence of up to 0.04 M urea.

Tissue Distribution Analysis—First-strand cDNAs were prepared from total RNAs (5 μg samples) of rabbit tissues as described above. The cDNAs were subjected to PCR in a 20-μl reaction mixture containing *Taq* DNA polymerase (1 unit), 0.5% dimethyl sulfoxide and primers (rgdh1 and rgdh2, 0.2 μM). The PCR product (10 μl) was run on a 1.0% (w/v) agarose gel and stained with ethidium bromide. Negative controls for each PCR included the RT template with no RNA or with no reverse transcriptase.

Subcellular fractionation of the rabbit liver homogenate was performed as described previously (*21*). For other tissues, 105,000 × *g* supernatant fractions of the homogenates were prepared as described above. The fractions were analyzed for protein and GDH activity. Protein concentrations were determined by the method of Bradford (*22*) using bovine serum albumin as the standard. The specific activities represent the means of determinations for two rabbits.

Other Analytical Methods—Isoelectric focusing on 7.5% (w/v) polyacrylamide disc gels (*23*) and analytical gel filtration on a Superdex 200 HR column (*21*) were carried out as described previously. A fluorescence emission spectrum of the enzyme (1 μM) was measured in 50 mM Mops, pH 7.0, containing 5 mM 2-ME at an excitation wavelength of 295 nm at 25°C using a Hitachi F-2000 spectrofluorometer. A circular dichroism spectrum of the enzyme in 10 mM Mops, pH 7.0, was measured between 240 and 190 nm at room temperature with a Jasco-720WI spectropolarimeter using 1-cm path cells. Protein sequence determination, including reductive pyridylethylation of the purified liver enzymes, their digestion with lysylendopeptidase, isolation of the peptides and sequencing by automated Edman degradation, was performed as described (*16*).

RESULTS

Purification and Sequence of Rabbit Liver GDH—GDH activity of 0.01 unit/mg was detected in the 105,000 × *g* supernatant fraction of the rabbit liver homogenate, but no detectable activity was present in the microsomal and mitochondrial fractions. GDH was purified from the rabbit liver cytosol by ammonium sulfate fractionation

Table 1. **Purification of GDH from rabbit liver.**

Step	Protein (mg)	Activity (units)	Specific activity (units/mg)	Yield (%)
Cytosol	4,300	45.9	0.011	100
$(NH_4)_2SO_4$ fractionation	3,910	41.3	0.011	90
Sephadex G-100	1,790	36.8	0.021	80
Q-Sepharose	66.6	16.5	0.247	36
Blue-Sepharose	4.1	10.2	2.49	22
Hydroxylapatite	3.2	8.2	2.56	18
Phosphate-cellulose	0.5	3.4	6.71	7

Table 2. **Substrate specificity of purified rabbit and human GDHs.**

Substrate	Rabbit liver GDH		Recombinant rabbit GDH		Recombinant human GDH	
	K_m (mM)	V_{max} (units/mg)	K_m (mM)	V_{max} (units/mg)	K_m (mM)	V_{max} (units/mg)
L-Gulonate	0.21	3.56	0.18	3.14	0.22	2.88
HBA	2.3	0.67	2.2	0.83	2.0	0.93
L-Threonate	2.9	0.10	1.2	0.12	2.1	0.10
NAD^+	0.011	3.68	0.010	3.09	0.010	2.86
$NADP^+$	0.89	0.23	0.67	0.34	0.52	0.21
Acetoacetate	8.3	1.04	9.9	1.67	9.9	1.23
NADH	0.0005	0.94	0.0006	1.61	0.0008	1.27

The kinetic constant for $NADP^+$ was determined with 40 mM L-gulonate, and those for acetoacetate and NADH were determined with 0.1 mM NADH and 40 mM acetoacetate, respectively.

and five column chromatographies, and representative results are summarized in Table 1. The purified GDH gave a single 36-kDa protein band on SDS-PAGE (Fig. 1) and was focused at pH 7.3 on gel isoelectric focusing. Gel exclusion chromatography on a Superdex 200 HR column resulted in a single peak corresponding to M_r = 70,000, demonstrating a dimeric structure for rabbit GDH.

Seven lysylendopeptidase-digested peptides of rabbit GDH were sequenced, although the N-terminal sequence of the enzyme could not be determined by direct Edman degradation. The peptide sequences perfectly matched regions of a sequence deduced from the cDNA for rabbit lens λ-CRY (*8*) (Fig. 2). Therefore, we isolated the λ-CRY cDNA from the total RNA preparation of rabbit liver by RT-PCR using primers that anneal the 5′- and 3′-ends of the coding region of the λ-CRY cDNA, and examined whether or not the recombinant protein exhibits GDH activity. The amplified cDNA encoded a 319–amino acid protein, which showed the same sequence as that reported for rabbit lens λ-CRY (*8*) except for lacking the codon for Glu^{309} of the lens λ-CRY. The extract of *E. coli* cells transfected with the expression plasmid harboring the cDNA contained a 36-kDa immunoreactive protein on Western blot analysis with the anti–rabbit GDH antibody (data not shown), and exhibited GDH activity (0.08 unit/mg). This immunoreactive protein and GDH activity were not detected in the extract of *E. coli* cells transfected with the vector alone. The recombinant GDH was purified to homogeneity from 1 liter of cultured cells, and 2.6 mg of enzyme was obtained, in a 22% yield, with a specific activity of 8.0 units/mg. In addition to the molecular weight and specific activity, the substrate specificity of the recombinant GDH was essentially identical to that of the rabbit liver enzyme (Table 2).

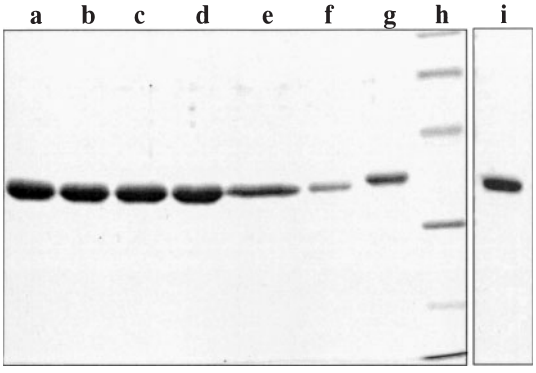

Fig. 1. **SDS-PAGE of purified GDHs.** Lanes: a, rabbit liver GDH (5 μg); b, recombinant rabbit GDH (5 μg); c, E157Q (5 μg); d, S124A (5 μg); e, N196Q (5 μg); f, D36R (2 μg); g, human recombinant λ-CRY (2 μg); h, molecular mass markers, and i, N196D (2 μg) run in a separate gel. The gels were stained with 0.2% Coomassie Brilliant Blue. Molecular masses of the markers are 97, 66, 45, 30, 20.1 and 14.4 kDa from the top.

Identity of GDH with λ-CRY—To determine whether or not GDH is identical to λ-CRY, we first assayed the GDH activities in rabbit tissues and amplified the λ-CRY cDNA from lens. The lens extract showed extremely high GDH activity, *i.e.* 430 munits/mg, compared with the activities in the other tissues: The activities (munits/mg) in kidney, liver, heart, lung, muscle, brain, testis and intestine extracts were 25, 11, 3.1, 2.8, 2.7, 2.6, 2.0 and 1.9, respectively. The tissue distribution of the activity correlated with the results for the expressed mRNA for GDH on RT-PCR analysis, in which the lens showed high expression (data not shown). We sequenced the five cDNA clones amplified from total RNA of lens, but no cDNA species with the codon for Glu^{309} was detected and all cDNAs encoded a protein comprising 319 amino acids with a sequence identical to that of rabbit GDH. Secondly, we isolated the cDNA for human λ-CRY, and characterized the recombinant protein, because Glu^{309} is not present in the sequences deduced from the cDNAs for λ-CRYs of human and other mammals (*9*). The extract of *E. coli* cells transfected with the expression plasmid harbor-

```
          1         10        20        30        40                  50        60        70        80
rCRY  MASPAAGDVLIVGSGLVGRSWAMLFASGGFRVKLYDIEPRQIT----GALENIRKEMKSLQQSGSLKGSLSAEEQLSLISSCTN
hCRY  MASSAAGCVVIVGSGVIGRSWAMLFASGGFQVKLYDIEQQQIR----NALENIRKEMKLLEQAGSLKGSLSVEEQLSLISGCPN
HAD   AKKIIVKHVTVIGGGLMGAGIAQVAAATGHTVVLVDQTEDILAKSKKGIEESLRKVAKKKFAENPKAGDEFVEKTLSTIATSTD
                                          45
          81        90        100       110       120       130       140       150       160
rCRY  LAEAVEGVVHIQECVPENLDLKRKIFAQLDSIVDDRVVLSSSSSCLLPSKLFTGLAHVKQCIVAHPVNPPYYIPLVELVP
hCRY  IQEAVEGAMHIQECVPEDLELKKKIFAQLDSIIDDRVILSSSTSCLMPSKLFAGLVHVKQCIVAHPVNPPYYIPLVELVP
HAD   AASVVHSTDLVVEAIVENLKVKNELFKRLDKFAAEHTIFASNTSSLQITSIANATTRQDRFAGLHFFNPVPVMKLVEVIK
                                                  137                 158       170
          161       170       180       190       200       210       220       230       240
rCRY  HPETSPATVDRTHALMRKIGQSPVRVLKEIDGFVLNRLQYAIISEAWRLVEEGIVSPSDLDLVMSDGLGMRYAFIGPLET
hCRY  HPETAPTTVDRTHALMKKIGQCPMRVQKEVAGFVLNRLQYAIISEAWRLVEEGIVSPSDLDLVMSEGLGMRYAFIGPLET
HAD   TPMTSQKTFESLVDFSKALGKHPV-SCKDTPGFIVNRLLVPYLMEAIRLYERGDASKEDIDTAMKLGAGYP---MGPFEL
                                          208
          241       250       260       270       280       290       300       310
rCRY  MHLNAEGMLSYSDRYSEGMKRVLKSFGSIPEFSGATVEKVNQAMCKKGPADPEHLAARREWRDECLKRELAKLKRQMQPQ 320
hCRY  MHLNAEGMLSYCDRYSEGIKHVLQTFGPIPEFSRATAEKVNQDMCMKVPDDPEHLAARRQWRDECLMR-LAKLKSQVQPQ 319
HAD   LDYVGLDTTKFIVDGWHEMDAENPLHQPSPSLNKLVAENKFGKKTGEGFYKYKLMLQLLRL 310
```

Fig. 2. **Alignment of the amino acid sequences of rabbit λ-CRY (rCRY), human λ-CRY (hCRY), and human HAD.** The deduced sequence of the isolated cDNA for rabbit GDH is the same as the rCRY sequence, except that it lacks Glu[309]. The numbering refers to amino acids in rCRY, in which the sequences of the peptides derived from the purified rabbit liver GDH are underlined. Dashes delineate spaces that are inserted to preserve optimal similarities of CRYs with human HAD. Of the coenzyme-binding residues (bold letters) and catalytically important residues (shaded bold letters) of human HAD, the residues corresponding to those of the present site-directed mutagenesis are shown with the amino acid numbers under the sequence.

ing the cDNA exhibited GDH activity of 0.037 unit/mg, and a homogeneous preparation with GDH activity of 5.6 units/mg was purified with a yield of 4% (Fig. 1). The human enzyme showed molecular masses of 36 and 70 kDa on SDS-PAGE and analytical gel filtration, respectively. The molecular masses and substrate specificity (Table 2) of the human enzyme are similar to those of the liver and recombinant GDHs of rabbit. The data indicate that GDH is identical to λ-CRY.

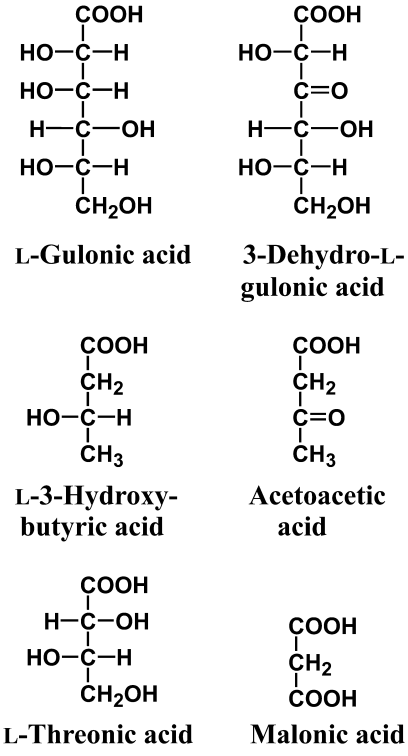

Fig. 3. **Structures of substrates, products and an inhibitor, malonic acid, of GDH.**

Properties of GDH—Maximal GDH activities of the recombinant rabbit and human GDHs were observed at pH 8.5–9.0, and their activities at pH 7.0 were 45% and 60% of the respective maximum rates. The enzymes also exhibited low dehydrogenase activity toward L-3-hydroxybutyrate (HBA) and L-threonate (Fig. 3), but did not oxidize 5–40 mM sugars or hydroxyacids (2-keto-L-gulonate, 3-deoxyglucosone, xylitol, L-threitol, ascorbic acid, malic acid, L-threonine, L-glycerate, L-tartarate and L-lactate), or 50 mM ethyl and methyl esters of 3-hydroxybutyrate. In the reverse reaction, the rabbit and human GDHs reduced acetoacetate in the presence of NADH and showed similar pH optima of around 6.5. When various carbonyl compounds were tested as substrates with rabbit GDH, 2,3-diketogulonate was reduced (K_m = 6.1 mM and V_{max} = 1.1 units/mg), but the enzyme was inactive toward 1 mM sugar derivatives (dehydroascorbate, 2-keto-L-gulonate, D-glucuronate and 3-deoxyglucosone), 5 mM esters (methyl and ethyl esters of acetoacetate, and malonic acid monoethyl ester), 10 mM ketoacids (pyruvate and oxaloacetate), and 1–5 mM other carbonyl compounds (methylglyoxal, 2,3-pentanedione, 3,4-hexanedione, camphorquinone and isatin). The rabbit and human enzymes utilized NAD(H) as the preferred coenzymes, as their K_m values for $NADP^+$ were high and no significant activity was detected with 0.1 mM NADPH as the coenzyme.

The activities of rabbit and human GDHs were completely inhibited by 10-min incubation with 1 μM *p*-chloromercuriphenylsulfonate. The inhibition was time-dependent, not decreased by dilution of the inhibitor–enzyme mixture, and not protected by the addition of 0.1 mM NAD^+ and 4 mM L-gulonate, suggesting that this reagent irreversibly binds to SH-groups other than the active centers of the enzymes. SH-protecting compounds,

Table 3. **Inhibition patterns and constants for malonate, products and Cibacron blue.**

Inhibitor	Varied substrate	Inhibition constant (mM)		Inhibition pattern
		K_{is}	K_{ii}	
Recombinant rabbit GDH				
Malonate	Gulonate	0.014	—	C
	NAD^+ [c]	—	0.17	UC
	HBA	0.013	—	C
	NAD^+	—	0.17	UC
Acetoacetate	HBA	3.9	9.8	NC
	NAD^+	—	10.3	UC
NADH	HBA	0.004	0.006	NC
	NAD^+	0.0002[a]	—	C
Cibacron blue	HBA	0.003	0.004	NC
	NAD^+	0.001[a]	—	C
Recombinant human GDH				
Malonate	Gulonate	0.001	—	C
	NAD^+	—	0.019	UC
NADH	NAD^+	0.0002[a]	—	C
Cibacron blue	NAD^+	0.001	—	C

K_{is} (slope effect) and K_{ii} (intercept effect) values were determined from replots of the slopes and intercepts, respectively, of double reciprocals plots in the presence of the inhibitor and fixed substrate, 1 mM NAD^+ or 10 mM HBA. The abbreviations of the inhibition patterns are: C, competitive; UC, uncompetitive; and NC, noncompetitive. [a]Standard errors were less than 33%; standard errors for other values were less than 15%.

such as 2-ME, dithiothreitol, glutathione and cysteine, did not affect the enzyme activities. Therefore, 2-ME was added to the buffers during the purification and storage of GDH. Rabbit and human GDHs were inhibited by malonate (IC_{50} values: 340 and 19 μM, respectively), which behaves as an instantaneous and reversible inhibitor (data not shown). The inhibition patterns of rabbit and human GDHs by malonate were competitive with respect to L-gulonate and uncompetitive with respect to NAD^+ (Table 3). Malonic acid monoethyl ester weakly inhibited the rabbit (IC_{50} = 5.5 mM) and human (IC_{50} = 0.20 mM) enzymes, but no significant inhibition (less than 15%) was observed by 1 mM L-ascorbate, monocarboxylic acids (L-glycolate, L-glycerate, propionate, pyruvate and *n*-butyrate), or dicarboxylic acids (oxalate, succinate, fumarate, maleate, oxaloacetate, α-ketoglutarate, malate and L-tartarate). The enzymes were not inhibited by 20 mM D-glucose, 2 mM 2-keto-L-gulonate, 1 mM metabolites of the uronate cycle (D-glucuronate, L-xylulose, xylitol and D-xylulose), or 6 mM nucleotides (ATP, ADP and AMP). Cibacron blue is known to bind to many oxidoreductases as a nucleotide analog (*24*), and showed competitive inhibition with respect to NAD^+.

Several salts stimulated the GDH activity of rabbit GDH at a saturating substrate concentration (Fig. 4a), whereas they were inhibitory at low substrate concentration (Fig. 4b). The dual effects were significant for P_i and pyrophosphate (PP_i), and there was no apparent difference in the effects between the sodium and potassium salts of P_i, suggesting the presence of binding site(s) for the P_i moiety on the enzyme. The effects of P_i and PP_i on the enzyme activity were pH-dependent. The two ions showed maximal stimulation and inhibition at pH 6.0–6.5, and the effects gradually decreased at higher pHs from 7.0 to 9.0. In double reciprocal plots of activity *versus* NAD^+ concentration, P_i acted as a non-essential activator (*25*) and a noncompetitive inhibitor in the presence of L-gulonate at 5 mM (Fig. 4c) and 0.5 mM (Fig. 4d), respectively, and did not significantly alter the K_m for NAD^+. Similar results were obtained when PP_i was added to the reaction mixtures (data not shown). Double reciprocal plots of activity versus L-gulonate concentration with increasing concentrations of P_i comprised a family of linear lines intersecting to the right of the $1/V$ axis, and replots of the apparent K_m, V_{max} and V_{max}/K_m (catalytic efficiency) *versus* P_i concentration yielded non-linear lines (Fig. 4e). Similar kinetic effects were also observed for PP_i (Fig. 4f). P_i and PP_i increased the K_m for the substrate more than V_{max}, resulting in a significant decrease in catalytic efficiency. The non-linear lines in the replots suggest that the enzyme possesses multiple binding sites for P_i or PP_i. The dual effects of P_i were observed for human GDH, and the addition of 5 mM P_i increased both K_m for L-gulonate (1.0 mM) and V_{max} (4.1 units/mg).

To explore further the mechanism of inhibition by P_i, the kinetic mechanism of the reaction catalyzed by rabbit GDH was examined by performing initial velocity measurement in the forward and reverse directions. HBA and acetoacetate were employed as the substrate and product pair, because dehydro-L-gulonate, the reduced product of L-gulonate was not available. Double reciprocal plots of initial velocity versus concentration of the varied substrate, HBA, at fixed levels of NAD^+ yielded a series of intersecting lines. Similar patterns of initial velocity were observed in the reverse reaction (data not shown). The results are consistent with a reaction mechanism that proceeds in a sequential manner. The results for product inhibition and dead-end inhibitors, malonate and Cibacron blue, are summarized in Table 3. The inhibition patterns are consistent with a sequential ordered mechanism, where NAD^+ binds to the enzyme first and NADH leaves last. The binding of the coenzymes to the enzyme was confirmed by significant quenching of the intrinsic fluorescence of rabbit GDH (λ_{max} = 330 nm) upon the addition of equimolar NAD^+ or NADH (data not shown).

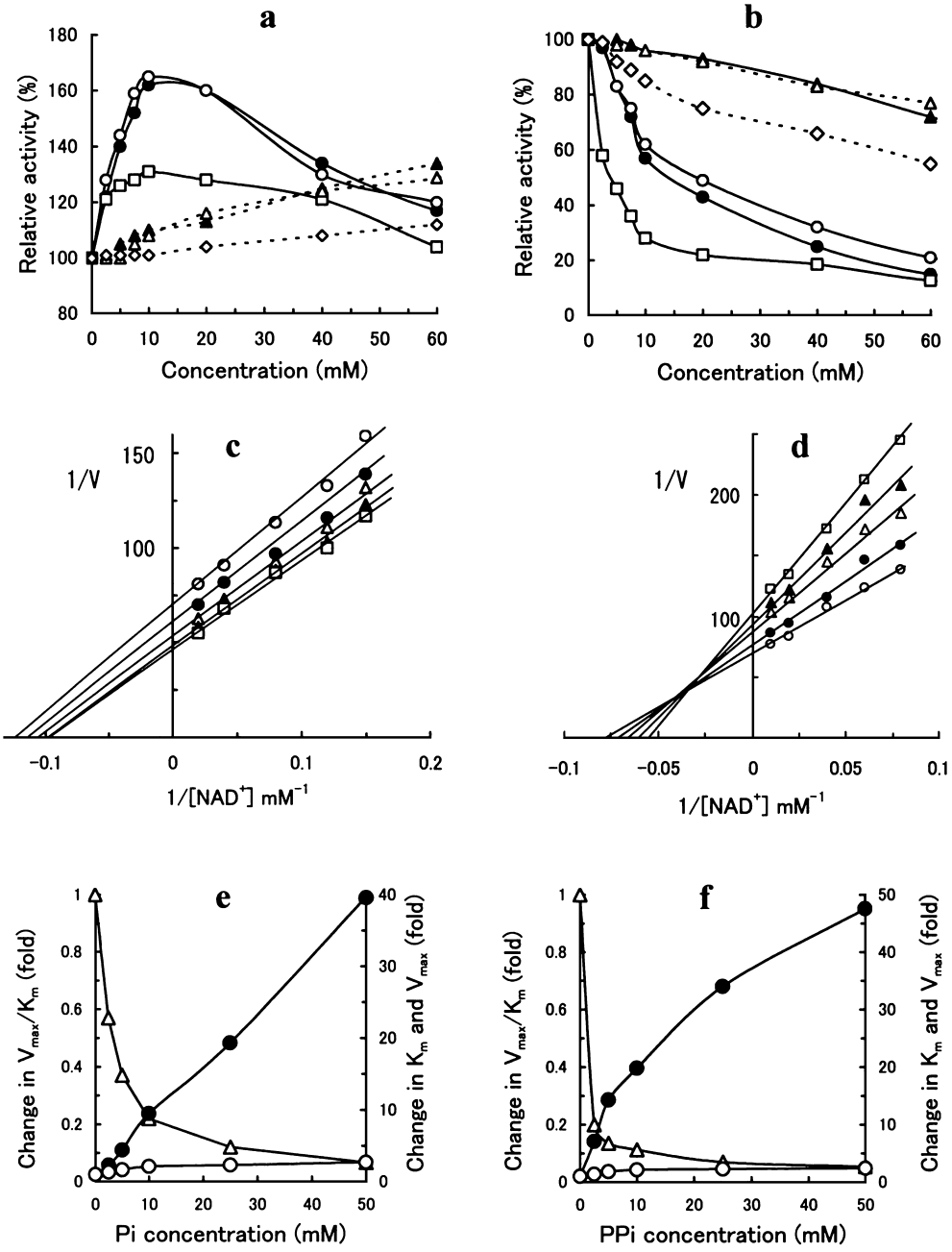

Fig. 4. **Effects of P_i and PP_i on the dehydrogenase activity of rabbit GDH.** a and b, the effects of salts on the activity in the presence of 4 mM (a) and 0.4 mM (b) L-gulonate. Salts: sodium P_i (open circles), potassium P_i (solid circles), sodium PP_i (open squares), NaCl (solid triangles), KCl (open triangles), and KNO_3 (open diamonds). c and d, double reciprocal plots of velocity versus NAD^+ concentration in the presence of 5 mM (c) and 0.5 mM (d) L-gulonate. Concentrations of sodium P_i (mM): 0 (open circles), 2.5 (solid circles), 5 (open triangles), 7.5 (solid triangles), and 10 (open squares). e and f, replots of the changes in the K_m for L-gulonate (solid circles), V_{max}, (open circles), and V_{max}/K_m (open triangles) on the addition of sodium P_i (e) and sodium PP_i (f). The kinetic constants were obtained from double reciprocal plots of velocity *versus* L-gulonate concentration, and are shown relative to the values in the absence of the ligands.

The kinetic constants, calculated from secondary plots of the initial velocity measurement data, were as follows: The Michaelis constants for NAD^+, HBA, NADH and acetoacetate were 9 ± 1, 2,000 ± 220, 0.5 ± 0.1 and 9,700 ± 110 μM, respectively; the dissociation constants for NAD^+ and NADH were 16 ± 3 and 0.4 ± 0.1 μM, respectively; and the V_{max} values for the oxidation and reduction were 0.92 ± 0.08 and 1.80 ± 0.2 units/mg, respectively. The results, together with the above effects of P_i or PP_i on the kinetic constants, suggest that the ion(s) bind at least to the free form and NAD(H)-binary complex of GDH in the kinetic pathway.

Stability—While no loss of GDH activity of the rabbit enzyme was observed in the pH range of 4.5 to 10.5 upon incubation for 30 min at 25°C, human GDH was stable in the narrower pH range of 6.0 to 10.0 (Fig. 5a). Rabbit GDH was gradually inactivated upon incubation at 48°C (Fig. 5b). The inactivation was prevented moderately by adding 10 mM P_i and completely by adding 1 mM NAD^+, but L-gulonate did not have any protective effect. The rabbit enzyme was rapidly inactivated upon incubation at 55°C, where the addition of both P_i and NAD^+ resulted in a greater protective effect than that of NAD^+ alone (Fig. 5c). Human GDH was more sensitive to heat treatment compared to rabbit GDH: Its activity rapidly decreased even upon incubation at 48°C (Fig. 5d). P_i exhibited a greater protective effect against the thermal inactivation of human GDH than NAD^+, and the protective effects of P_i and NAD^+ were synergetic. The human enzyme was completely inactivated within 1 min upon incubation at 55°C, and no protective effects of P_i and the coenzyme were detected (data not shown). P_i and NAD^+

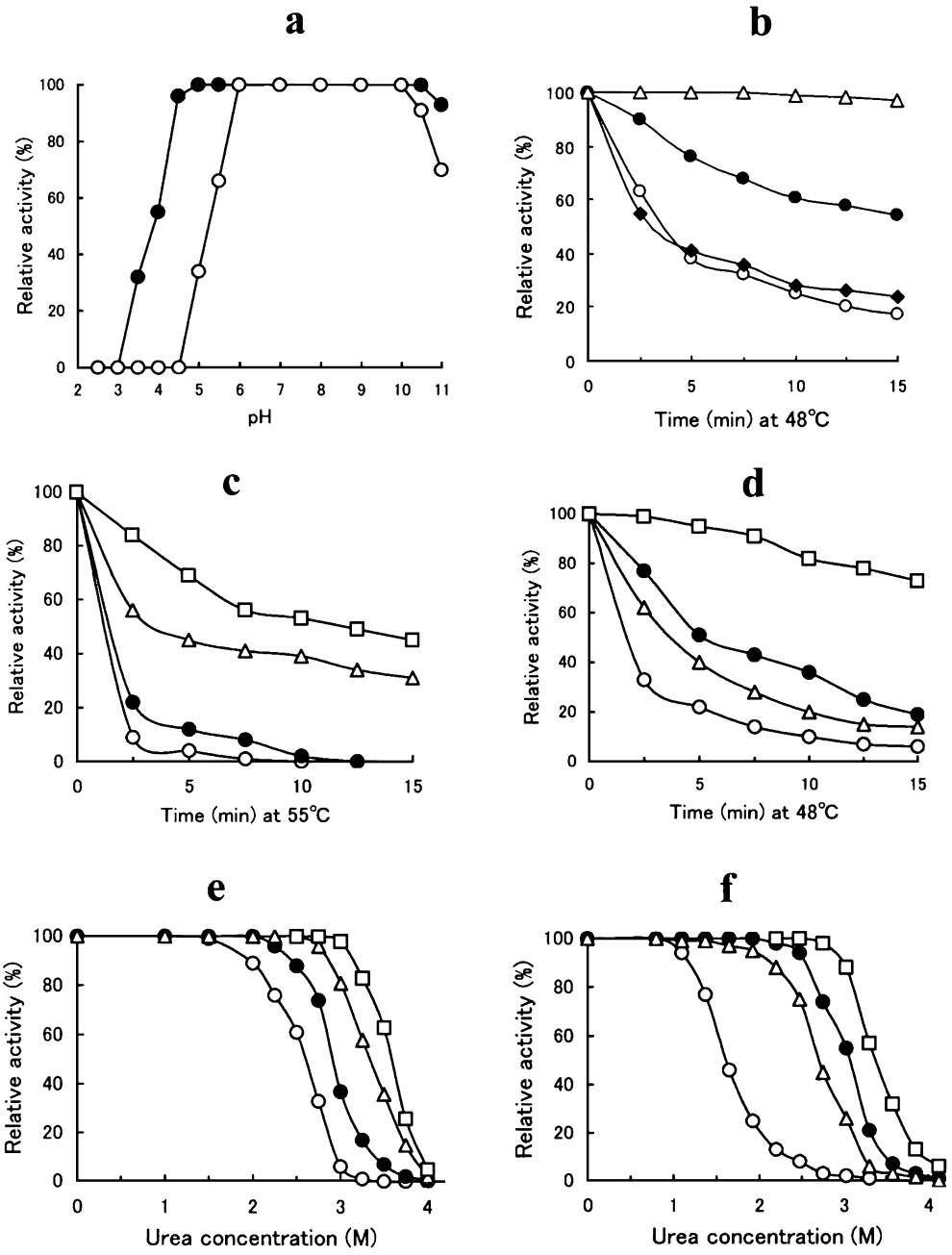

Fig. 5. **Stability of rabbit and human GDHs.** a, pH stability of rabbit (solid circles) and human (open circles) GDHs. b and c, stability of rabbit GDH at 48°C (b) and 55°C (c). d, stability of human GDH at 48°C. e and f, stability of rabbit (e) and human (f) GDHs against urea denaturation. The stability was examined in the absence (open circles) or presence of the following ligands: 1 mM NAD^+ (open triangles), 10 mM sodium P_i (solid circles), and 1 mM NAD^+ plus 10 mM sodium P_i (open squares).

also displayed protective effects against urea denaturation of the enzymes, to which rabbit GDH was more stable than the human enzyme (Fig. 5, e and f).

Kinetic Alteration by Mutagenesis—The NAD^+-linked activity in the extract of *E. coil* cells expressing the D36R mutant of rabbit GDH was low (0.4 munit/mg), but 3-fold higher activity was observed with $NADP^+$ as the coenzyme. The extract of *E. coil* cells expressing the E157Q mutant exhibited NAD^+-linked GDH activity (54 munits/mg), whereas the activity in the extract expressing the S124A mutant was low (0.1 munit/mg) and no activity was detected in extracts of cells expressing the H145Q, N196Q or N196D mutants. The mutant GDHs were purified in yields of 1–3 mg per 1-liter culture of *E. coil* cells. Each eluted as a single peak at a position of approximately 70 kDa from the Sephadex G-100 column and gave a single 36-kDa protein band on SDS-PAGE (Fig. 1), demonstrating the dimeric structures of the mutant enzymes. The circular dichroism spectra of the mutant enzymes were essentially identical to that of the wild-type (data not shown), indicating that none of these mutations causes major changes in the overall secondary structure.

The D36R mutation resulted in a great increase in the K_m for NAD^+ and a small decrease in the K_m for $NADP^+$ (Table 4). The V_{max}/K_m value for $NADP^+$ was higher (9.5-fold) than that for NAD^+, although the V_{max}/K_m values for L-gulonate of the two reactions were the same because of the concomitant increase in the K_m for the substrate. No GDH activity was detected for the H145Q, N196Q and N196D mutants even when high concentrations (20 μg) of the purified enzymes were used, but the addition of equal

Table 4. **Kinetic parameters for L-gulonate (Gul) oxidation by purified mutant enzymes.**

Parameter[a]	D36R	D36R/WT	E157Q	E157Q/WT	S124A	S124A/WT
NAD^+-linked activity						
K_m NAD^+	1.3[b]	144	0.069	7	0.033	4
K_m Gul	14[c]	78	0.49	3	4.4	24
V_{max}	1.34	0.4	4.20	1	0.14	0.04
V_{max}/K_m NAD^+	1.0	0.003	61	0.2	4.2	0.01
V_{max}/K_m Gul	0.09	0.006	8.57	0.5	0.032	0.002
$NADP^+$-linked activity						
K_m $NADP^+$	0.20[b]	0.3	0.64[b]	1	nd	–
K_m Gul	18.5[d]	8	18.5[d]	8	nd	–
V_{max}	1.9	5	0.32	0.9	0.002[e]	–
V_{max}/K_m $NADP^+$	9.5	17	0.50	0.9	nd	–
V_{max}/K_m Gul	0.10	0.7	0.017	0.1	nd	–

[a] K_m, V_{max} and V_{max}/K_m are expressed in mM, units/mg and units/mg/mM, respectively. [b] The fixed substrate is 40 mM Gul. [c] The fixed coenzyme is 5.0 mM NAD^+. [d] The fixed coenzyme is 4.0 mM $NADP^+$. [e] Specific activity determined with 4.0 mM $NADP^+$ and 40 mM Gul. nd, the value could not be determined because of low activity.

amounts of NADH quenched the intrinsic fluorescence of the two mutant enzymes to a level similar to those observed in the cases of the wild-type and the other mutant enzymes (data not shown). The S124A mutation decreased V_{max} (22-fold), and increased K_m values for both NAD^+ (4-fold) and L-gulonate (24-fold), resulting in a more than 100-fold decrease in the catalytic efficiency. In addition, this mutant showed high sensitivity to malonate (K_{is} = 1.2 ± 0.3 μM). On the other hand, the E157Q mutation did not result in large changes in the kinetic constants for the $NAD(P)^+$-linked forward reactions and malonate inhibition (K_{is} = 10 ± 1 μM). Even in the reverse reaction, the K_m for acetoacetate and V_{max} values of this mutant were 18 mM and 0.61 unit/mg, respectively, which are changes of less than 3-fold compared with the values for the wild-type enzyme (Table 2). The effect of P_i on the kinetic constants appeared not to be altered by the S124A and E157Q mutations. The K_m for L-gulonate and V_{max} values determined in the presence of 5 mM P_i were 29 mM and 1.83 units/mg, respectively, for the S124A enzyme, and the respective values were 2.4 mM and 5.49 units/mg for the E157Q enzyme. Both the S124A and E157Q mutations slightly impaired the thermostability of the enzyme (Fig. 6).

DISCUSSION

The present characterization of rabbit liver GDH and recombinant proteins encoded in the cDNAs for rabbit and human λ-CRYs indicate that the two proteins are identical. Although rabbit λ-CRY was reported to be composed of 320 amino acids with an additional Glu at position 309 (*8*), our results of cDNA isolation clearly show that one mRNA species coding for a protein of 319 amino acids without Glu^{309} is expressed in both rabbit lens and liver. The high expression of GDH/λ-CRY in rabbit lens implies that GDH is recruited as a structural and refractive protein without gene duplication in the tissue. The increase in stability of GDH by binding P_i and NADH may be related to why the rabbit selects this protein as a taxon-specific CRY. In the lenses of several animals including rabbit, NAD(P)H exists at high concentrations and has been suggested to function as a filter for UV radiation (*26*, *27*). The high affinity of GDH for NADH suggests an additional role in the maintenance of reduced coenzyme at high concentrations in rabbit lens. On the other hand, λ-CRY is not highly expressed in the lenses of other animal species (*8*), in which it may have non-refractive function(s). Recently, an NADH-dependent dehydroascorbate reductase in rabbit lens was suggested to be identical or related to λ-CRY (*28*). However, rabbit GDH and human λ-CRY exhibit significant activity only for L-gulonate and structurally related organic acids with a 3-hydroxy or 3-keto group, and do not reduce dehydroascorbate or other dicarbonyl compounds. In the lenses of animals other than rabbit, GDH may contribute to osmoregulation by producing xylitol, as this role has been proposed in bovine and rat lenses (*2*).

The λ-CRY mRNA has been reported to be expressed in non-lenticular tissues of rabbit and other animal species (*8*, *9*), and in rabbit liver, the result of Western blot analysis suggests that λ-CRY is a mitochondrial protein (*8*). However, there is no mitochondrial targeting signal in the sequences of λ-CRYs. In fact, GDH, which is idential to λ-CRY, localizes in the cytosolic fraction of rabbit liver homogenates, and the hepatic enzymes in pig (*3*) and

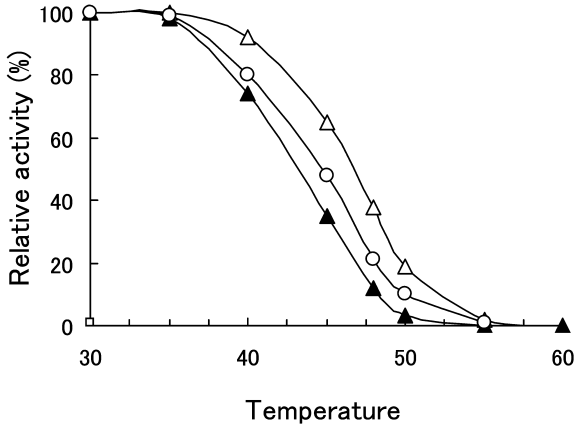

Fig. 6. **Thermostability of the wild-type and mutant enzymes.** The wild-type (6 μg/ml, open triangles), and S124A (32 μg/ml, open circles) and E157Q (6 μg/ml, solid triangles) mutants were treated for 5 min at the indicated temperatures.

chicken (*29*) are also cytosolic. Thus, GDH is a cytosolic protein in non-lenticular tissues, and functions as an enzyme in the uronate cycle, as evidenced by the substrate specificity of rabbit and human GDHs. The K_m values for L-gulonate and NAD^+ of rabbit and human GDHs are almost the same, but are much lower than the respective values of 5.1 mM and 40 μM of the pig liver enzyme (*3*), which were determined in 0.1 M Tris-HCl, pH 8.5, in the presence of 1 mM cysteine. As we have shown, the GDH activities of rabbit and human GDHs are affected by several ions, and rabbit GDH shows a high K_m for L-gulonate (1.5 mM) when the assay is performed in 0.1 M Tris-HCl, pH 8.5. The kinetic constants of the pig enzyme might be low under assay conditions using low concentrations of buffer and at physiological pH. The most important finding of this study is the decrease in the catalytic efficiency of GDH by physiological concentrations of P_i. This may indicate a mechanism whereby an increase in P_i, as a result of energy drain and hydrolysis of ATP, would result in lowering of the metabolic rate of the uronate cycle, and redirection of glucose metabolism from the production of UDP-glucuronate and xylitol to glycolysis to restore the ATP level. The proposed metabolic regulation is relevant, because the uronate cycle accounts for about 5% of the total glucose catabolized per day in humans (*30*). In addition, in animals with the ability to synthesize ascorbate, the branched pathway of the uronate cycle might be stimulated by elevation of the L-gulonate concentration under cellular conditions involving high P_i concentrations.

The kinetic analysis of the effect of P_i on the enzyme activity of GDH, together with its ability to protect the enzyme against inactivation by heat and urea, suggest that the effector binds to both the free and NAD(H)-complex forms of the enzyme, which has multiple P_i binding sites. Judging from the pH dependence of the inhibition by P_i and its pK_a value, $H_2PO_4^-$ probably binds to the binding sites of the enzyme. The binding site(s) for P_i may be near the substrate-binding site, but not near the coenzyme-binding site, because the addition of P_i mostly affects the K_m for the substrate. The site-directed mutagenesis of Ser^{124} and Glu^{157} suggests that other residues are involved in the binding of P_i, and further structural studies are needed to elucidate the chemical steps of the effects by P_i.

Malonate was found to be a novel potent inhibitor of both rabbit and human GDHs. The inhibition patterns of malonate with respect to the coenzyme and substrate, together with the decrease in the K_{is} value caused by the S124A mutation, indicate that malonate binds to the substrate binding site of the enzyme. That analogs of malonate, including its ethyl monoester, cause little or no inhibition suggests that there is a site that fits the small tricarbon dicarboxylic acid in the substrate-binding pocket of the enzyme. Since substantial concentrations (maximum 192 nmol/g tissue) of free malonate are detected in rat brain, liver and kidney after birth (*31*), malonate may act as an inhibitor of GDH, although the physiological relevance of the inhibition remains unknown.

GDH shows low sequence similarity with NAD^+-dependent HAD. In the crystal structure of the human HAD binary complex with NAD^+ (*10*), the N-terminal 200 residues form an NAD^+-binding domain, in which hydroxyl groups of the adenine ribose of the coenzyme interact with the carboxyl group of Asp^{45} (Fig. 7) and the side-chain of Gln^{46}. Asp^{45}, but not Gln^{46}, is conserved in GDH at position 36 (Fig. 2), and thus Asp^{36} is expected to play a critical role in the coenzyme specificity for NAD(H). In many pyridine nucleotide–dependent enzymes, the critical determinant for the NAD(H) specificity is a negatively charged residue, usually Asp, at the C-terminus of the second β strand of the βαβ fold, whereas that for NADP(H) specificity is a positively charged residue that forms salt bridges with the 2′-phosphate of NADP(H) (*32–35*). The importance of this residue is demonstrated by the inversion of the coenzyme specificity of rabbit GDH due to the D36R mutation, in which the concomitant increase in K_m for L-gulonate and decrease in the V_{max} value caused by the D36R mutation may result from a subtle change in orientation of the coenzyme due to the introduction of the larger side chain of Arg in place of that of the Asp.

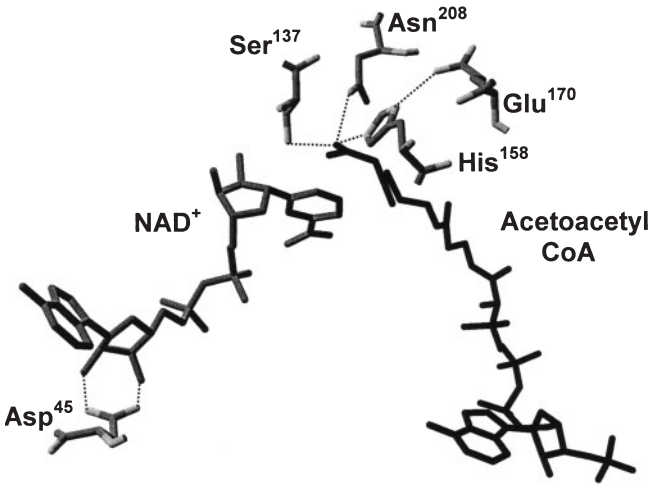

Fig. 7. **Active-site residues and Asp^{45} in the ternary complex of human HAD with NAD^+ and a substrate, acetoacetyl CoA.** Dash lines represent possible hydrogen bonding interactions between the carbonyl group of the substrate and the side-chains of Ser^{137}, His^{158} and Asn^{208}, as well as between the side-chains of His^{158} and Glu^{170} of the enzyme (*11*). The carboxylate group of Asp^{45} forms a bifurcated hydrogen bond with the hydroxyl group of the adenine ribose of the coenzyme. The figure was created with Swiss-Pdb Viewer (*38*).

A crystallographic study on human HAD (*11*) proposed its catalytic mechanism, in which Ser^{137} interacts with the substrate, coenzyme and His^{158}, a catalytic base, and Glu^{170} neutralizes the positive charge on His^{158} after hydrogen transfer (Fig. 7). In addition, the side-chain amide of Asn^{208} is thought to interact with the dehydrogenated carbonyl group of the substrate. The proposed roles of His^{158} and Glu^{170} are supported by the site-directed mutagenesis studies with a homologous enzyme, HAD in *E. coli* multiple complex of fatty acid oxidation, in which substitutions of the two residues with Gln result in significant decreases in k_{cat} values (*36*, *37*). The mutation of the residue equivalent to Glu^{170} in human HAD also greatly reduces the thermostability of HAD in the *E. coli*

multiple complex (*37*). The two residues correspond to His^{145} and Glu^{157} in rabbit GDH (Fig. 2). The H145Q mutation in GDH yields an inactive enzyme form with the ability to bind NAD(H), indicating that this residue plays a critical role in the catalysis by the enzyme. However, the small effects of the E157Q mutation on the kinetic constants and thermostability of rabbit GDH are not in agreement with the drastic decrease in k_{cat} and great impairment of the stability on mutagenesis of the corresponding residue of HAD in the *E. coli* enzyme complex. This clearly indicates that the role of the conserved Glu differs between GDH and HAD. Although the roles of Ser^{137} and Asn^{208} in HAD have not been examined by site-directed mutagenesis, the large effects of the mutations of equivalent residues, Ser^{124} and Asn^{196}, in GDH on the activity can be expected if the catalytic mechanism of GDH is similar to that of HAD. The large alterations of K_m for L-gulonate, V_{max} and catalytic efficiency caused by the S124A mutation in GDH suggest the importance of the OH group of Ser^{124} in the catalytic reaction. The complete inactivation by the mutation of Asn^{196} into Gln or Asp is unexpected, because the corresponding residue of HAD, Asn^{208}, is thought to stabilize the reaction product together with Ser^{137} in the proposed catalytic mechanism for human HAD. The result suggests that the side-chain amide of Asn^{196} is more critical in the catalytic mechanism of GDH than the hydroxyl group of Ser^{124}.

The present data on the mutagenesis of Asp^{36}, His^{145} and Ser^{124} indicate that GDH is a member of the HAD family, but suggest that the roles of the conserved Glu^{157} and Asn^{196} in the catalytic mechanism differ between GDH and HAD. A recent homology search using human GDH/λ-CRY as a probe in protein databases indicated that this family comprises 27 proteins, although the functions of most members are unknown (*9*). In addition to the functional characterization of the new members of this family, further studies on the roles of the above and other residues conserved among members are required to determine whether or not the proteins with similar sequences are indeed identical in terms of their catalytic mechanism.

REFERENCES

1. Nakagawa, J., Ishikura, S., Asami, J., Isaji, T., Usami, N., Hara, A., Sakurai, T., Tsuritani, K., Oda, K., Takahashi, M., Yoshimoto, M., Otsuka, N., and Kitamura, K. (2002) Molecular characterization of mammalian dicarbonyl/L-xylulose reductase and its localization in kidney. *J. Biol. Chem.* **277**, 17883–17891
2. Goode, D., Lewis, M.E., and Crabbe, M.J. (1996) Accumulation of xylitol in the mammalian lens is related to glucuronate metabolism. *FEBS Lett.* **395**, 174–178
3. Smiley, J.D. and Ashwell, G. (1961) Purification and properties of β-L-hydroxy acid dehydrogenase. II. Isolation of β-keto-L-gluconic acid, an intermediate in L-xylulose biosynthesis. *J. Biol. Chem.* **236**, 357–364
4. Bublitz, C. and Lehninger, A.L. (1961) The role of aldonolactonase in the conversion of L-gulonate to L-ascorbate. *Biochim. Biophys. Acta* **47**, 288–297
5. Roberts, B.D., Bailey, G.D., Buess, C.M., and Carper, W.R. (1978) Purification and characterization of hepatic porcine gluconolactonase. *Biochem. Biophys. Res. Commun.* **84**, 322–327
6. Bailey, G.D., Roberts, B.D., Buess, C.M., and Carper, W.R. (1979) Purification and partial characterization of beef liver gluconolactonase. *Arch. Biochem. Biophys.* **192**, 482–488
7. Carper, W.R., Mehra, A.S., Campbell, D.P., and Levisky, J.A. (1982) Gluconolactonase: a zinc containing metalloprotein. *Experientia* **38**, 1046–1047
8. Mulders, J.W., Hendriks, W., Blankesteijn, W.M., Bloemendal, H., and de-Jong, W.W. (1988) λ-Crystallin, a major rabbit lens protein, is related to hydroxyacyl coenzyme A dehydrogenases. *J. Biol. Chem.* **263**, 15462–15466
9. Chen, J., Yu, L., Li, D., Gao, Q., Wang, J., Huang, X., Bi, G., Wu, H., and Zhao, S. (2003) Human CRYL1, a novel enzyme-crystallin overexpressed in liver and kidney and downregulated in 58% of liver cancer tissues from 60 Chinese patients, and four new homologs from other mammalians. *Gene* **302**, 103–113
10. Barycki, J.J., O'Brien, L.K., Bratt, J.M., Zhang, R., Sanishvili, R., Strauss, A.W., and Banaszak, L.J. (1999) Biochemical characterization and crystal structure determination of human heart short chain L-3-hydroxyacyl-CoA dehydrogenase provide insights into catalytic mechanism. *Biochemistry* **38**, 5786–5798
11. Barycki, J.J., O'Brien, L.K., Strauss, A.W., and Banaszak, L.J. (2000) Sequestration of the active site by interdomain shifting. Crystallographic and spectroscopic evidence for distinct conformations of L-3-hydroxyacyl CoA dehydrogenase. *J. Biol. Chem.* **275**, 27186–27196
12. Borack, L.I. and Sofer, W. (1971) *Drosophila* β-L-hydroxyacid dehydrogenase. Purification and properties. *J. Biol. Chem.* **246**, 5345–5350
13. Doner, L.W. and Hicks, K.B. (1981) High-performance liquid chromatographic separation of ascorbic acid, erythrobic acid, dehydroascorbic acid, dehydroerythrobic acid, diketogulonic acid and diketogluconic acid. *Anal. Biochem.* **115**, 225–230
14. Khadem, H.D.E., Horton, D., Meshreki, M.H., and Nashed, M.A. (1971) New route for the synthesis of 3-deoxyaldos-2-uloses. *Carbohydr. Res.* **17**, 183–192
15. Sambrook, J., Fritsch, E.F., and Maniatis, T. (1989) In *Molecular Cloning: A Laboratory Manual*, 2nd edition, Cold Spring Harbor Laboratory Press, New York.
16. Nakanishi, M., Deyashiki, Y., Ohshima, K., and Hara, A. (1995) Cloning, expression and tissue distribution of mouse tetrameric carbonyl reductase. Identity with an adipocyte 27-kDa protein. *Eur. J. Biochem.* **228**, 381–387
17. Laemmli, U.K. (1970) Cleavage of structural proteins during the assembly of the head of bacteriophage. *Nature* **227**, 680–685
18. Towbin, H., Staehelin, T., and Gordon, J. (1979) Electrophoretic transfer of proteins from polyacrylamide gels to nitrocellulose sheets: Procedure and some applications. *Proc. Natl Acad. Sci. USA* **76**, 4350–4354
19. Harwood, H.J.Jr., Greene, Y.J., and Stacpoole, P.W. (1986) Inhibition of human leukocyte 3-hydroxy-3-methylglutaryl coenzyme A reductase activity by ascorbic acid. An effect mediated by the free radical monodehydroascorbate. *J. Biol. Chem.* **261**, 7127–1735
20. Cleland, W.W. (1963) The Kinetics of enzyme-catalyzed reactions with two or more substrates or products. I. Nomenclature and equations. *Biochim. Biophys. Acta* **67**, 104–137
21. Ishikura, S., Usami, N., Kitahara, K., Isaji, T., Oda, K., Nakagawa, J., and Hara, A. (2001) Enzymatic characteristics and subcellular distribution of a short-chain dehydrogenase/reductase family protein, P26h, in hamster testis and epididymis. *Biochemistry* **40**, 214–224
22. Bradford, M.M. (1976) A rapid and sensitive method for the quantitation of microgram quantities of protein utilizing the principle of protein-dye binding. *Anal. Biochem.* **72**, 248–254
23. Hara, A., Deyashiki, Y., Nakagawa, M., Nakayama, T., and Sawada, H. (1982) Isolation of proteins with carbonyl reductase activity and prostaglandin-9-ketoreductase activity from chicken kidney. *J. Biochem.* **92**, 1753–1762
24. Thompson, S.T., Cass, K.H., and Stellwagen, E. (1975) Blue Dextran-Sepharose: An affinity column for the dinucleotide fold in proteins. *Proc. Natl Acad. Sci. USA* **72**, 669–672
25. Segel, I.H. (1975) In *Enzyme Kinetics*, pp. 227–272, John Wiley & Sons, New York

26. Zigler, J.S. and Rao, P.V. (1991) Enzyme/crystallins and extremely high pyridine nucleotide levels in the eye lens. *FASEB J.* **5**, 223–225
27. Tomarev, S.I. and Piatigorsky, J. (1996) Lens crystallins of invertebrates—diversity and recruitment from detoxification enzymes and novel proteins. *Eur. J. Biochem.* **235**, 449–465
28. Suzuki, T., Bando, M., Oka, M., Tsukamoto, H., Akatsuka, I., Kawai, K., Obazawa, H., Kobayashi, S., and Takehana, M. (2003) λ-Crystallin related to dehydroascorbate reductase in the rabbit lens. *Jpn. J. Ophthalmol.* **47**, 437–443.
29. Herzberg, G.R. and Gad, M. (1984) Evidence that the cytosolic activity of 3-hydroxybutyrate dehydrogenase in chicken liver is L-3-hydroxyacid dehydrogenase. *Biochim. Biophys. Acta* **802**, 67–70
30. Hollmans, S. and Touster, O. (1964) In *Non-Glycolytic Pathways of Metabolism of Glucose*, pp. 107–113, Academic Press, New York/London
31. Mitzen, E.J. and Koeppen, A.H. (1984) Malonate, malonyl-coenzyme A, and acetyl-coenzyme A in developing rat brain. *J. Neurochem.* **43**, 499–506
32. Tanaka, N., Nonaka, T., Nakamura, K.T., and Hara, A. (2001) SDR: structure, mechanism of action, and substrate recognition. *Cur. Org. Chem.* **5**, 89–111
33. Carugo, O. and Argos, P. (1997) NADP-dependent enzymes. I: Conserved stereochemistry of cofactor binding. *Proteins* **28**, 10–28
34. Clermont, S., Corbier, C., Mely, Y., Gerard, D., Wonacott, A., and Branlant, G. (1993) Determinants of coenzyme specificity in glyceraldehyde-3-phosphate dehydrogenase: role of the acidic residue in the fingerprint region of the nucleotide binding fold. *Biochemistry* **32**, 10178–10184
35. Bellamacina, C.R. (1996) The nicotinamide dinucleotide binding motif: A comparison of nucleotide binding proteins. *FASEB J.* **10**, 1257–1269
36. He, X.-Y. and Yang, S.-Y. (1996) Histidine-450 is the catalytic residue of L-3-hydroxyacyl coenzyme A dehydrogenase associated with the large α-subunit of the multienzyme complex of fatty acid oxidation from *Escherichia coli*. *Biochemistry* **35**, 9625–9630
37. He, X.-Y., Deng, H., and Yang, S.-Y. (1997) Importance of the γ-carboxyl group of glutamate-462 of the large α-subunit for the catalytic function and the stability of the multienzyme complex of fatty acid oxidation from *Escherichia coli*. *Biochemistry* **36**, 261–268
38. Guex, N. and Peitsch, M.C. (1997) SWISS-MODEL and Swiss-Pdb Viewer: an environment for comparative protein modeling. *Electrophoresis* **18**, 2714–2723